Positioning and Trajectory Following Tasks in Microsystems Using Model Free Visual Servoing

Erol Ozgur, Mustafa Unel
Faculty of Engineering and Natural Sciences, Sabanci University
Orhanli Tuzla 34956, Istanbul, TURKEY
Email: erol@su.sabanciuniv.edu, munel@sabanciuniv.edu

***Abstract*— In this paper, we explore model free visual servoing algorithms by experimentally evaluating their performances for various tasks performed on a microassembly workstation developed in our lab. Model free or so called uncalibrated visual servoing does not need the system calibration (microscope-camera-micromanipulator) and the model of the observed scene. It is robust to parameter changes and disturbances. We tested its performance in point-to-point positioning and various trajectory following tasks. Experimental results validate the utility of model free visual servoing in microassembly tasks.**

I. Introduction

Fabrication of tiny devices has become extremely important and much recent work has focussed on how to manipulate and assemble microparts using microassembly strategies. Microassembly lies between conventional (macro-scale) assembly, parts with dimensions greater than one millimeter, and the emerging field of nanoassembly that contain parts on the molecular scale, i.e. less than a micrometer [1]. Since microassembly is a relatively new area and suffers from several problems such as inefficiency, unreliability, less throughput and high costs, it has induced the evolution of visually guided microrobotic systems to overcome such issues. In order to ensure desired properties, the real-time visual feedback control or so called visual servoing strategies can effectively and economically be used in microrobotic systems.

As detailed in [2], visual servoing strategies can be classified into two broad categories: position-based and image-based visual servoing. In position-based visual servoing, the error is defined in the task space which necessitates estimation of the pose with known camera and manipulator model, while image-based one does not need estimation of the pose. Image-based approach is robust to system modeling and camera calibration errors and computationally efficient, since the error is defined over the features on the image plane. Image Jacobian matrix was introduced by Weiss in image-based visual servoing to relate changes in image features to changes in the pose [3]. To compute image Jacobian one needs calibration of the system which is not always an easy task.

Model free or so called uncalibrated visual servoing provides an online estimation to the Jacobian matrix without any knowledge of the optical and robotic system. So far it has been mostly used in macro domain robotic applications. However, it can provide more flexibility in microsystems since the calibration of the optical system is a tedious and error prone process, and recalibration is required at each focusing level of the optical system. Hosoda and Asada have estimated the Jacobian matrix using an extended least squares algorithm with exponential data weighting [4]. Jagersand employed a Broyden's method in the Jacobian estimation [5]. Piepmeier used a recursive least squares (RLS) estimate and a dynamic Quasi-Newton method for model free visual servoing [6]-[7]. Qian exploited the Kalman filtering technique to estimate the Jacobian elements [8]. Lv has employed the Kalman filtering with fuzzy logic adaptive controller to ensure stable Jacobian estimation [9].

In this paper, we employ a specific model free visual servoing algorithm [6]-[7] in experiments on a microassembly workstation developed in our microsystem lab and evaluate its performance for various positioning and trajectory following tasks. Model free visual servoing which we employ in this paper, consists of a recursive least-square (RLS) dynamic Jacobian estimator proposed by Piepmeier in [6]-[7], and two different controllers: a Dynamic Gauss-Newton controller [6]-[7] and an Optimal controller similar to the one in [10].

The remainder of this paper is organized as follows: In Section II, we briefly describe the visual tasks to be performed. Visual tracking is also explained in this section. Section III presents dynamic Jacobian estimation and visual controllers for image based visual servoing. Section IV is on experimental results and discussions. Finally Section V concludes the paper with some remarks.

II. Visual Task Description and Tracking

We would like to locate a microgripper with respect to a static target or to make it follow desired trajectories by controlling its velocity using model free visual servoing. In order to perform these tasks we shall need to measure, in the image plane, the motion of the features related to the microgripper. This necessitates a tracking algorithm which must be efficient, accurate and robust in order to track features in real-time or near video rate. In this work, we used the efficient second-order minimization (ESM) algorithm [11] which is based on minimizing the sum-of-squared-differences (SSD) between a given template image and the current image. Theoretically, amongst all standard minimization algorithms, the Newton method has the highest local convergence rate since it is based on a second-order Taylor series of the SSD. However, the Hessian computation in the Newton method is

time consuming. In addition, if the Hessian is not positive definite, convergence problems occur. The ESM method has two main advantages. First, it has a convergence rate similar to the Newton method, but the ESM does not need to compute the Hessian because it uses only first order derivatives, and second it avoids local minima close to the global one. It is shown that ESM has a higher convergence rate than other minimization techniques. The algorithm is intrinsically robust to partial occlusion and illumination changes. Strong camera displacements can be handled in real-time by the ESM visual tracking. A more complete description of the algorithm and its implementation can be found in [11].

III. Model Free Visual Servoing

We consider image-based visual servoing where the error signal that is directly measured in the image is mapped to the robot actuators' command input. Visual controllers are designed to determine the joint velocities.

A. Background and Problem Formulation

Let $\theta \in \Re^n$, $f \in \Re^m$ and $x \in \Re^6$ denote the vectors of joint variables, image features obtained from visual sensors and the pose of end-effector, respectively. The relation between θ and x is $x = x(\theta)$. Differentiating it with respect to time implies

$$\dot{x} = J_R(\theta)\dot{\theta} \tag{1}$$

where $J_R(\theta) = \partial x/\partial\theta \in \Re^{6\times n}$ is the robot Jacobian which describes the relation between the robot joint velocities and the velocities of its end-effector in Cartesian space. The relation between f and x is given as $f = f(x)$ and its differentiation with respect to time yields

$$\dot{f} = J_I(x)\dot{x} \tag{2}$$

where $J_I(x) = \partial f/\partial x \in \Re^{m\times 6}$ is the image Jacobian which describes the differential relation of the image features and position and orientation of the robot end-effector. The composite Jacobian is defined as

$$J = J_I J_R \tag{3}$$

where $J \in \Re^{m\times n}$ is a matrix which is the product of image and robot Jacobian. Thus, the relation between joint coordinates and image features is given by

$$\dot{f} = J\dot{\theta} \tag{4}$$

The error function in the image plane for a moving target at position $f^*(t)$ and an end-effector at position $f(\theta)$ is given as

$$e(\theta, t) = f(\theta) - f^*(t) \tag{5}$$

where $f^*(t)$ represents desired image features at time t.

B. Dynamic Jacobian Estimation

Since the system (micrgripper and optical microscope) model is assumed to be unknown, a recursive least-squares (RLS) algorithm [6] is used to estimate the composite Jacobian J. This is accomplished by minimizing the following cost function, which is a weighted sum of the changes in the affine model over time,

$$\varepsilon_k = \sum_{i=0}^{k-1} \lambda^{k-i-1} \|\Delta m_{ki}\|^2 \tag{6}$$

where

$$\Delta m_{ki} = m_k(\theta_i, t_i) - m_i(\theta_i, t_i) \tag{7}$$

with $m_k(\theta, t)$ being an expansion of $m(\theta, t)$, which is the affine model of the error function $e(\theta, t)$, about the k^{th} data point as follows:

$$m_k(\theta, t) = e(\theta_k, t_k) + \hat{J}_k(\theta - \theta_k) + \frac{\partial e_k}{\partial t}(t - t_k) \tag{8}$$

In light of (8), (7) becomes

$$\Delta m_{ki} = e(\theta_k, t_k) - e(\theta_i, t_i) - \frac{\partial e_k}{\partial t}(t_k - t_i) - \hat{J}_k h_{ki}, \tag{9}$$

where $h_{ki} = \theta_k - \theta_i$, the weighting factor λ satisfies $0 < \lambda < 1$, and the unknown variables are the elements of $\hat{J}_k$.

Solution of the minimization problem yields the following recursive update rule for the composite Jacobian:

$$\hat{J}_k = \hat{J}_{k-1} + (\Delta e - \hat{J}_{k-1} h_\theta - \frac{\partial e_k}{\partial t} h_t)(\lambda + h_\theta^T P_{k-1} h_\theta)^{-1} h_\theta^T P_{k-1} \tag{10}$$

where

$$P_k = \frac{1}{\lambda}(P_{k-1} - P_{k-1} h_\theta (\lambda + h_\theta^T P_{k-1} h_\theta)^{-1} h_\theta^T P_{k-1}) \tag{11}$$

and $h_\theta = \theta_k - \theta_{k-1}$, $h_t = t_k - t_{k-1}$, $\Delta e = e_k - e_{k-1}$, and $e_k = f_k - f_k^*$, which is the difference between the end-effector position and the target position at k^{th} iteration. The term $\frac{\partial e_k}{\partial t}$ predicts the change in the error function for the next iteration, and in the case of a static camera it can directly be estimated from the target image feature vector with a first-order difference:

$$\frac{\partial e_k}{\partial t} \cong -\frac{f_k^* - f_{k-1}^*}{h_t} \tag{12}$$

The weighting factor is $0 < \lambda \leq 1$ and when close to 1 results in a filter with a longer memory. The Jacobian estimate is used in the visual controllers to determine the joint variables θ_k that track the target.

C. Design of Visual Controllers

1) Dynamic Gauss-Newton Controller: The dynamic Gauss-Newton method [6] minimizes the following time varying objective function

$$E(\theta, t) = \frac{1}{2} e^T(\theta, t) e(\theta, t) \tag{13}$$

By minimizing above objective function it computes the joint variables iteratively as follows:

$$\theta_{k+1} = \theta_k - (\hat{J}_k^T \hat{J}_k)^{-1} \hat{J}_k^T (e_k + \frac{\partial e_k}{\partial t} h_t) \quad (14)$$

Control is defined as

$$u_{k+1} = \dot{\theta}_{k+1} = -K_p \hat{J}_k^{\dagger} (e_k + \frac{\partial e_k}{\partial t} h_t) \quad (15)$$

where K_p and $\hat{J}_k^{\dagger}$ are some positive proportional gain and the pseudo-inverse of the estimated Jacobian at k^{th} iteration, respectively.

2) Optimal Controller: Equation (4) can be discretized as

$$f(\theta_{k+1}) = f(\theta_k) + T \hat{J}_k u_k \quad (16)$$

where T is the sampling time of the vision sensor and $u_k = \dot{\theta}_k$ is the velocity vector of the end effector. An optimal control law as in [10] can be developed based on the minimization of an objective function, which penalizes the pixelized position errors and the control energy as:

$$E_{k+1} = [f_{k+1} - f_{k+1}^*]^T Q [f_{k+1} - f_{k+1}^*] + u_k^T L u_k \quad (17)$$

where Q and L are the weighting matrices. The resulting optimal control input u_k can be derived as

$$u_k = -(T \hat{J}_k^T Q T \hat{J}_k + L)^{-1} T \hat{J}_k^T Q [f_k - f_{k+1}^*] \quad (18)$$

Since there is no standard procedure to compute the weighting matrices Q and L, they are adjusted to obtain desired transient and steady state response.

IV. Experiments

A. System Setup

Our microassembly workstation consists of a Nikon SMZ1500 optical stereomicroscope that has a CCD camera module adapter onto which a Basler A602fc camera with $9.9\mu m \times 9.9\mu m$ cell sizes is mounted. The microscope has 1.6X objective and additional zoom. Zoom levels can be varied between 0.75X-11.25X, implying $15:1$ zoom ratio. Fig. 1 shows the complete microassembly system. The gripper that was used in the experiments is a Zyvex microgripper with an opening gap of $100\mu m$ and it is rigidly fastened to a PI M-111.1 high-resolution micro-translation stage with $50nm$ incremental motion in x, y and z positioning axes (see Fig. 2). The controllers for linear stages were implemented on dSpace ds1005 motion control board which steers the microgripper. The visual tracking algorithm (ESM) accomplished to track a 50×50 window up to 250 pixels/sec velocity at 33 Hz.

B. Tasks

Experiments were conducted on our microassembly station and visual feedback has been provided through coarse visual path of the microscope. In experiments, visual servoing was accomplished with dynamic Gauss-Newton and Optimal controllers for micropositioning and trajectory following tasks at 1X and 4X zoom levels. Fig. 3 depicts the microgripper for two different zoom levels.

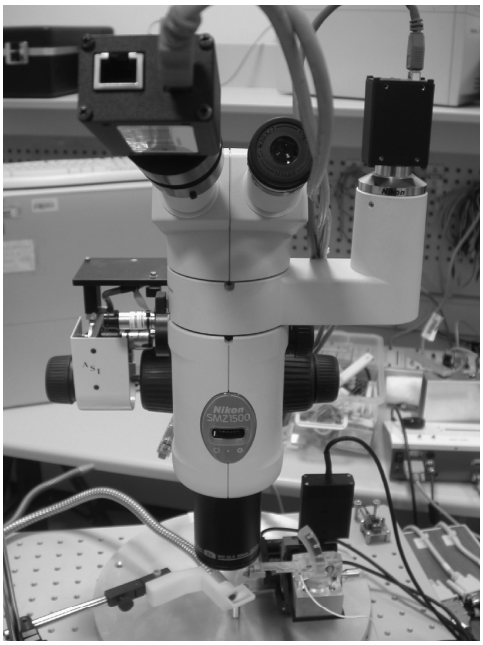

Fig. 1. Microassembly workstation and attached visual sensors

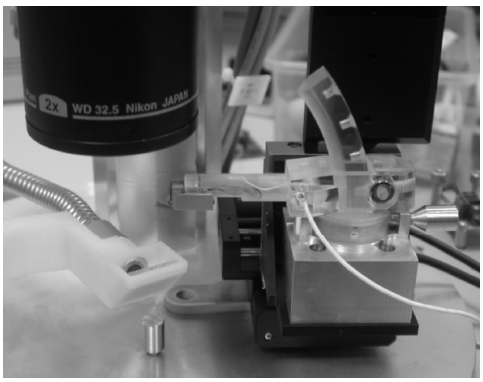

Fig. 2. Microgripper mounted on linear stages in assembly workspace

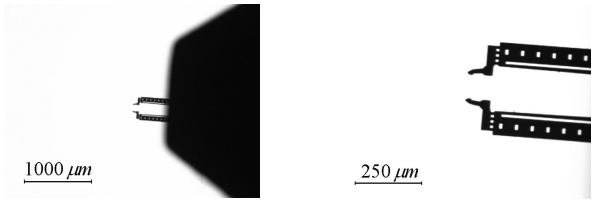

Fig. 3. Views of microgripper at 1X and 4X

Last two columns of Table I show the area in mm^2 of the microscopic view and the effective pixel size (resolution) for the zoom levels indicated in the first column. All experimental outcomes were assessed in terms of accuracy and precision. Accuracy and precision values were determined as the mean and the standard deviation of the error-norms. To estimate initial microscopic system Jacobian, each linear stage is successively moved by a small amount and the change of

microgripper position in image is used to build its components. The microgripper is then servoed in workspace for a while to ensure convergence of the Jacobian to its true values.

TABLE I

Z	$Area$ (mm^2)	ΔP (μm)
1X	4×3	6.18
4X	1×0.75	1.55

1) Micropositioning: In this task the microgripper was sent to a desired position from an arbitrary initial position by giving step inputs of 50 pixels both in x and y directions as references. This corresponds to 70.8 pixels from the initial position. Results of these experiments for the Dynamic Gauss-Newton and the Optimal control, are tabulated in Tables II and III where Z, $\{K_p,\ Q,\ L\}$, $Step$, t_s, $Acc.$ and $Prec.$ represent zoom level, control gains, step input, settling time, accuracy and precision, respectively. The positioning errors were calculated after the response was settled and remained in 3% of its final value. Figs. 4 and 5 demonstrate the step responses and the corresponding Optimal control signals for a trial under 1X and 4X zoom levels .

TABLE II

DYNAMIC GAUSS-NEWTON CONTROL RESULTS FOR MICROPOSITIONING

Z	K_p	$Step$ (pix)	t_s (sec)	$Acc.$ (μm)	$Prec.$ (μm)
1X	4	50	1.6	4.37	1.32
4X	2	50	3	2.81	1.44

TABLE III

OPTIMAL CONTROL RESULTS FOR MICROPOSITIONING

Z	Q	L	$Step$ (pix)	t_s (sec)	$Acc.$ (μm)	$Prec.$ (μm)
1X	0.9	0.05	50	1.6	8.60	3.65
4X	0.6	0.4	50	1.6	4.74	1.92

2) Trajectory Following: Apart from micropositioning, the same model free visual servoing was tested in trajectory following tasks with square, circle and sine trajectories. A linear interpolator was used to generate midway targets to make the microgripper pursue them along these reference trajectories. The upshots for these trials are depicted in Tables IV and V. The tracking error was computed as the distance between the microgripper and the current midway target at each frame. Figs. 6, 7 and 8 depict results of trajectory following experiments and the error-norms versus time graphs. Performance versus microassembly tasks for two controllers are also depicted in Figs. 9 and 10 where each ellipse defines the accuracy (center of the ellipse) and the precision (half length of the major axis of the ellipse) of the performed task.

C. Discussions

It can be seen from the presented tables and graphs that model free visual servoing performs positioning and trajectory

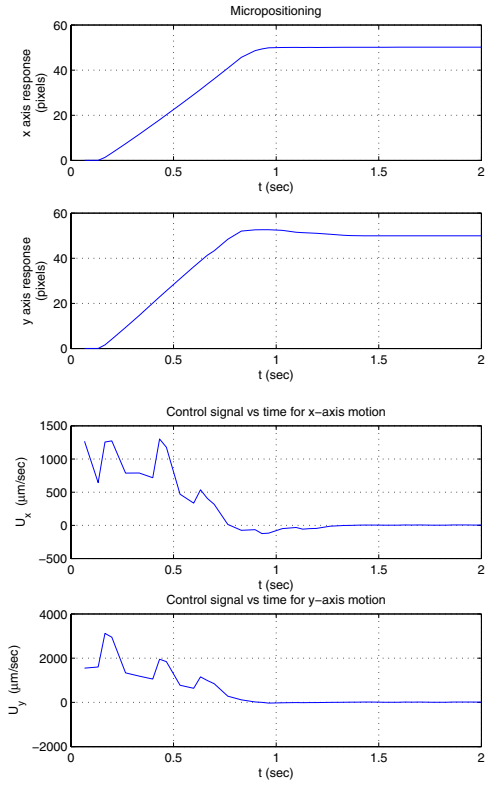

Fig. 4. Step responses and optimal control signals at 1X

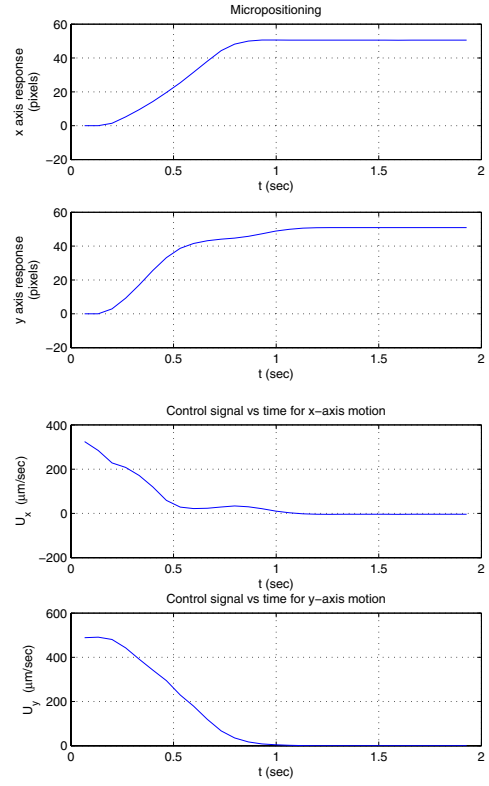

Fig. 5. Step responses and optimal control signals at 4X

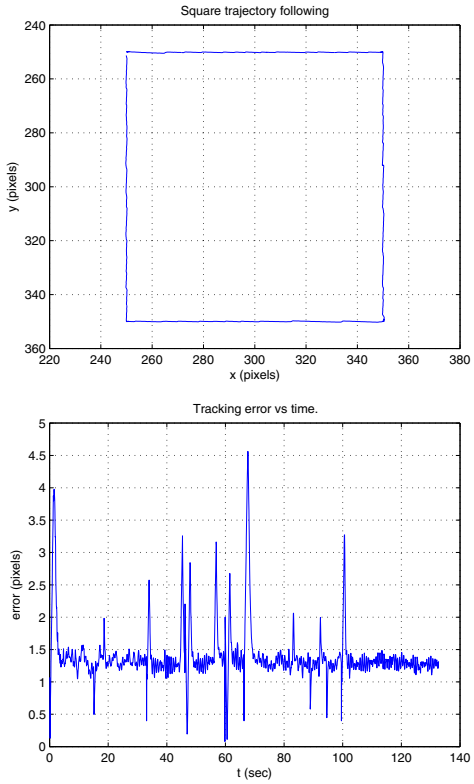

Fig. 6. Square trajectory and the tracking error using optimal control at 1X

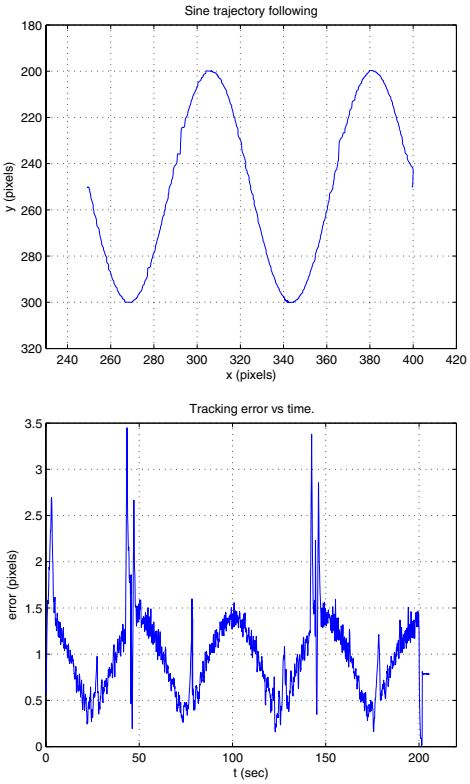

Fig. 8. Sine trajectory and the tracking error using optimal control at 1X

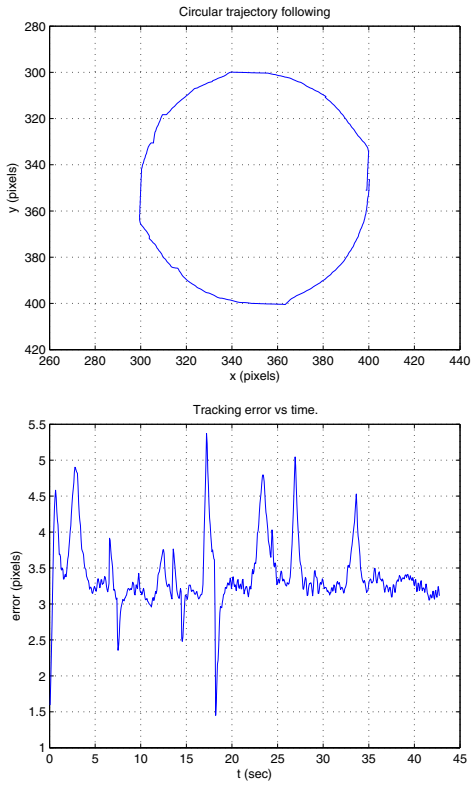

Fig. 7. Circle trajectory and the tracking error using optimal control at 1X

TABLE IV

DYNAMIC GAUSS-NEWTON CONTROL RESULTS FOR TRAJECTORY FOLLOWING

Z	(μm)	Square	Circle	Sine
1X	Acc.	3.78	24.87	11.36
	Prec.	3.43	4.62	5.87
4X	Acc.	1.45	6.08	2.86
	Prec.	1.45	2.95	1.85

TABLE V

OPTIMAL CONTROL RESULTS FOR TRAJECTORY FOLLOWING

Z	(μm)	Square	Circle	Sine
1X	Acc.	8.65	21.05	6.14
	Prec.	2.70	2.90	2.74
4X	Acc.	1.64	3.30	1.17
	Prec.	1.12	1.17	0.57

following tasks with micron accuracies. On the average, the tasks were achieved with $5\mu m$ and $3\mu m$ accuracies for positioning and with $12\mu m$ and $3\mu m$ accuracies for trajectory following at 1X and 4X zoom levels, respectively. Upon comparison of controllers, we see that the performance of Dynamic Gauss-Newton is better than the Optimal control in linear motions (positioning and square trajectory following) while Optimal controller performs better than the previous one in nonlinear motions (circle and sine trajectory following). Furthermore, task precision for Dynamic Gauss-Newton control is worse than that of Optimal control at both zoom levels. If time considerations are important for the tasks, uncalibrated

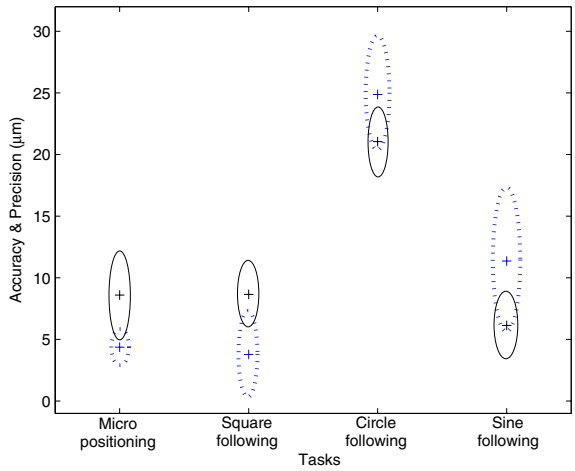

Fig. 9. Accuracy & precision ellipses for Dynamic Gauss-Newton (dotted) and Optimal (solid) controllers at 1X

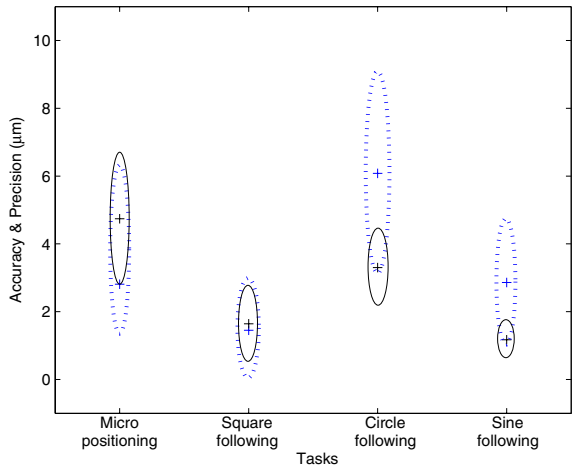

Fig. 10. Accuracy & precision ellipses for Dynamic Gauss-Newton (dotted) and Optimal (solid) controllers at 4X

visual servoing is more sluggish than the calibrated one.

V. Conclusion

In this paper, we have investigated and experimentally validated the use of model free visual servoing in micropositioning and trajectory following tasks. Model free servoing has the advantages of carrying out a task without requiring a model of the system and adapting itself to different operating modes through a dynamic estimation of the composite Jacobian. Experimental results show that positioning and trajectory following tasks can be performed in a robust manner with micron accuracies. The performance of model free visual servoing has been evaluated with two different controllers. It has been observed that for linear motion Dynamic Gauss-Newton controller shows slightly better performance, while Optimal controller does better job for the rest of the trajectories. Since the objective of this study was to demonstrate the potential of model free visual servoing in microworld with the advantages it has in macro domain, we did not try to force the limits of visual servoing.

Acknowledgement

Authors gratefully acknowledge the support provided by SU Internal Grant No. IACF06 – 00417.

References

[1] Bohringer, Karl F., Ronald S. Fearing, and Ken Y. Golberg. "The Handbook of Industrial Robotics." 2 nd ed. Berkeley , CA : Shimon Nof, Wiley & Sons 1998.

[2] S. Hutchinson, G. D. Hager, and P. I. Corke, "A tutorial on visual servo control," IEEE *Trans. on Robotics and Automation*, vol. 12, no. 5, pp. 651-670, 1996.

[3] L. Weiss, A. C. Sanderson, and C. Neuman, "Dynamic sensor-based control of robots with visual feedback," IEEE *Journal of Robotics and Automation*, vol. 3, no. 5, pp. 404-417, 1987.

[4] K. Hosoda, M. Asada, "Versatile visual servoing without knowledge of true Jacobian," in Proc. IEEE/RSJ *Int. Conf. on Intelligent Robots and Systems*, pp. 186-193, 1994.

[5] M. Jagersand, 0. Fuentes, and R. Nelson, "Experimental evaluation of uncalibrated visual servoing for precision manipulation," in Proc. IEEE *Int. Conf. on Robotics and Automation*, pp. 2874-2880, 1997.

[6] J. A. Piepmeier, H. Lipkin, "Uncalibrated Eye-in-Hand Visual Servoing", *The International Journal of Robotics Research*, 2003.

[7] J. A. Piepmeier, G. V. McMurray, and H. Lipkin, "Uncalibrated dynamic visual servoing," IEEE *Trans. on Robotics and Automation*, vol. 20, no.1, pp. 143-147, 2004.

[8] J. Qian and J. Su, "Online Estimation of Image Jacobian Matrix by Kalman-Bucy Filter for Uncalibrated Stereo Vision Feedback", *International Conference on Robotics & Automation*, 2002.

[9] Xiadong Lv and Xinhan Huang, "Fuzzy Adaptive Kalman Filtering based Estimation of Image Jacobian for Uncalibrated Visual Servoing", Proc. IEEE/RSJ *International Conference on Intelligent Robots and Systems*, 2006.

[10] Stephen J. Ralis, Barmeshwar Vikramaditya, and Bradley J. Nelson, "Micropositioning of A Weakly Calibrated Microassembly System Using Coarse-to-Fine Visual Servoing Strategies", *IEEE Trans. On Electronics Packing Manufacturing*, 2000.

[11] S. Benhimane and E. Malis, "Real-time image-based tracking of planes using efficient second-order minimization", IEEE/RSJ*International Conference on Intelligent Robots Systems*, Sendai, Japan, October 2004.